FIELD QUALITY MEASUREMENTS IN THE FNAL TWIN-APERTURE 11 T DIPOLE FOR LHC UPGRADES*

T. Strauss, G. Apollinari, E. Barzi, G. Chlachidze, J. Di Marco, F. Nobrega, I. Novitski, S. Stoynev, D. Turrioni, G. Velev, A.V. Zlobin#, FNAL, Batavia, IL 60510, USA
B. Auchmann, S. Izquierdo Bermudez, M. Karppinen, L. Rossi, F. Savary, D. Smekens
CERN, CH-1211 Geneva 23, Switzerland

Abstract

FNAL and CERN are developing an 11 T Nb_3Sn dipole suitable for installation in the LHC to provide room for additional collimators. Two 1 m long collared coils previously tested at FNAL in single-aperture dipole configuration were assembled into the twin-aperture configuration and tested including magnet quench performance and field quality. The results of magnetic measurements are reported and discussed in this paper.

INTRODUCTION

The development of the 11 T Nb_3Sn dipole for the LHC collimation system upgrade, started in 2011 as a collaborative effort of FNAL and CERN magnet teams [1]. The recent R&D status of the project was reported in [2]. A single-aperture 2-m long dipole demonstrator and two 1-m long dipole models have been assembled and tested at FNAL in 2012-2014. The 1 m long collared coils were then assembled into the twin-aperture configuration and tested in 2015-2016 [3]. The first magnet test was focused on the quench performance of twin-aperture magnet configuration including magnet training, ramp rate sensitivity and temperature dependence of magnet quench current [4]. In the second test performed in July 2016 field quality in one of the two magnet apertures has been measured and compared with the data for the corresponding single-aperture model. These results are reported and discussed in this paper.

MAGNET DESIGN AND PARAMETERS

The design concepts of FNAL 11 T Nb_3Sn dipole in single- and twin-aperture configurations are described in [1, 5]. Fabrication details and performance parameters of the two configurations are compared in [3, 6].

Magnet design is based on two-layer coils, stainless steel collar and cold iron yoke supported by strong stainless steel skin. The twin-aperture magnet MBHDP01 consists of two collared coils inside a common iron yoke with coils 5 and 7 around one aperture and coils 9 and 10 around the other aperture. Coil position inside the yoke and coil electrical connections in the twin-aperture magnet MBHDP01 are shown in Fig. 1. The coils 5 and 7 and the coils 9 and 10 were previously tested in single-aperture dipole models MBHSP02 and MBHSP03 respectively.

* Work supported by Fermi Research Alliance, LLC, under contract No. DE-AC02-07CH11359 with the U.S. Department of Energy and European Commission under FP7 project HiLumi LHC, GA no.284404
# zlobin@fnal.gov

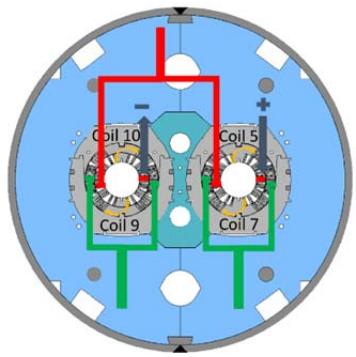

Figure 1: Coil layout and connetion inside the yoke.

MAGNETIC FIELD MEASUREMENT

MBHDP01 was tested at the FNAL Vertical Magnet Test Facility. Magnetic measurements were performed using 26 mm and 130 mm long, and 26 mm wide 16-layer Printed Circuit Board (PCB) probes [7]. The probe rotation speed was 1 Hz. The resolution of magnetic measurements is estimated better than 0.5 unit. The rotating coil system was installed in the aperture with coils 9 and 10.

The field induction B in magnet aperture was represented in terms of harmonic coefficients defined in a series expansion using the complex functions

$$B_y + iB_x = B_1 10^{-4} \sum_{n=1}^{\infty} (b_n + ia_n) \left(\frac{x+iy}{R_{ref}} \right)^{n-1}, \quad (1)$$

where B_x and B_y are horizontal and vertical field components in the Cartesian coordinate system, b_n and a_n are $2n$-pole normal and skew harmonic coefficients at the reference radius R_{ref}=17 mm.

RESULTS AND DISCUSSION

Figures 2-4 show the dependences of the magnet Transfer Function ($TF=b_1/I$) and low-order "normal" (b_2, b_3, b_4, b_5) and "skew" (a_2, a_3) field harmonics measured in MBHDP01 and MBHSP03 vs. the magnet current. The measurement data are compared with 2D and 3D calculations of geometrical harmonics and iron saturation effect in the twin-aperture MBHDP01 using ROXIE [8].

The measurements were done in current loops with the current ramp rate of 20 A/s. The effect of eddy currents on the field quality was studied previously in single-aperture models MBHSP02 and 03 by performing measurements in current loops with current ramp rates up to 80 A/s. It was found that this effect it small thanks to

the stainless steel core in the cable [6]. It is not discussed in this paper.

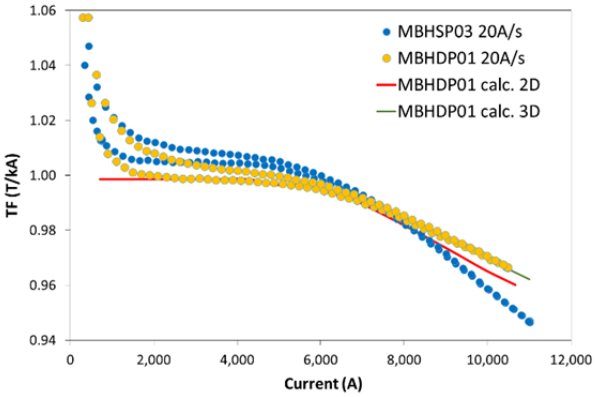

Figure 2: Transfer function *TF* vs. magnet current.

The large hysteresis (persistent current effect) is seen at low currents in the *TF* and the allowed harmonics b_3 and b_5. It is due to the large size of Nb_3Sn sub-elements D_{eff} and high critical current density J_c of the used Nb_3Sn strand. It was already shown [3, 8] that this effect is in a good agreement with calculations based on both ROXIE [9] and OPERA 2D codes except for the coil re-magnetization part below the injection field which needs to be better understood. Some hysteresis is also seen in the non-allowed normal and skew low-order harmonics. It is likely due to the asymmetry of magnet geometry and variations of coil magnetization.

The iron saturation effect is observed in *TF,* b_2 and little bit in b_3 above 4 kA. This effect as well as the geometrical harmonics are in a reasonably good agreement (except for the geometrical a_2 and b_3) with 3D ROXIE calculations based on the yoke length, cross-section geometry and magnetic properties.

Figure 5 shows axial variations of the normal b_2 and skew a_2 quadrupole measured with 130-mm and 26-mm long coils at the magnet current of 6 kA. The detailed z-scan in MBHSP03 with the short coil revealed harmonics oscillations with a period comparable with the cable transposition pitch. These oscillations indicate on the non-uniform current distribution in the cable cross-section. This non-uniform current distribution could be a cause of the large degradation of magnet quench current observed in FNAL 11 T dipole models [3]. Measurements performed in MBHDP01 and MBHSP03 with the long coil and large step average the data and, thus, hide these oscillations.

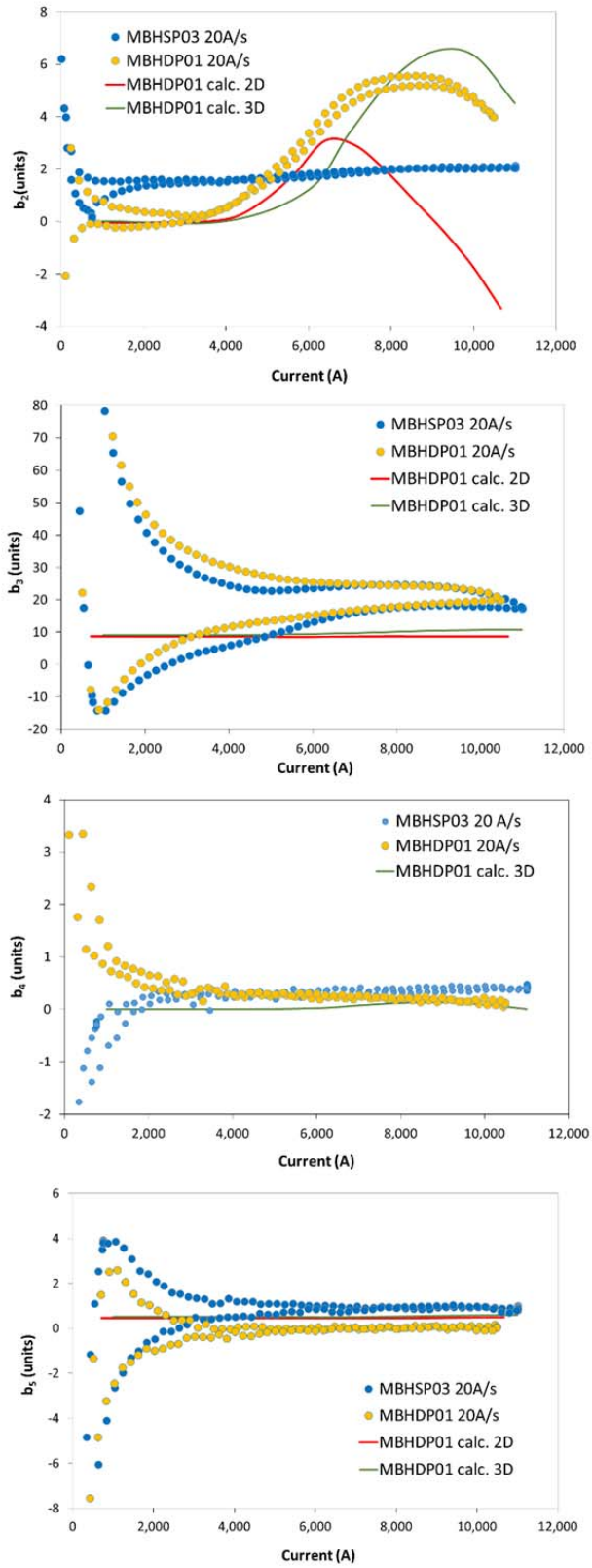

Figure 3: Normal quadrupole b_2, sextupole b_3, octupole b_4 and decapole b_5 vs. magnet current.

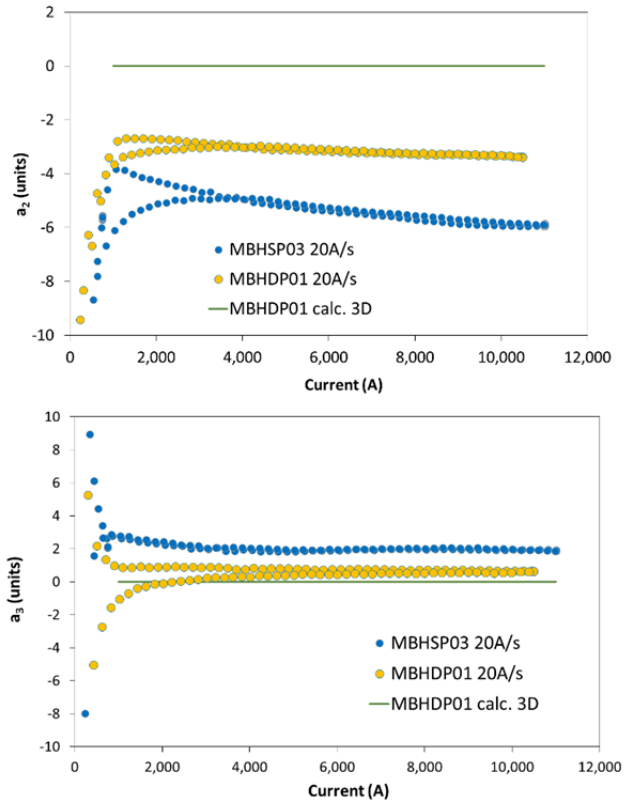

Figure 4: Skew quadrupole a_2 and sextupole a_3 vs. magnet current.

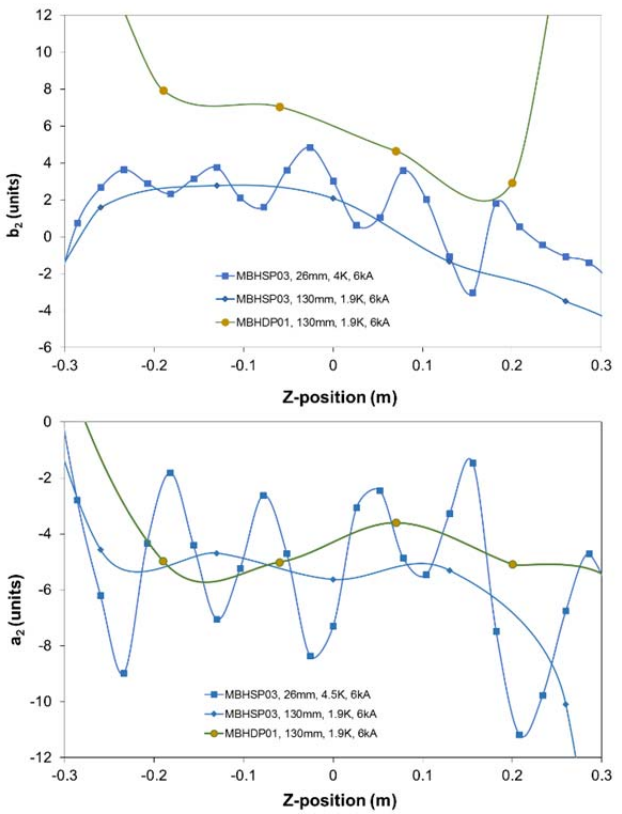

Figure 5: Variations of b_2 and a_2 along the magnet axis.

Table 1: Geometrical Harmonics at 3.5 kA

n	MBHSP03		MBHDP01	
	a_n	b_n	a_n	b_n
2	-4.6	1.4	-3.5	0.6
3	2.0	16.1	0.4	20.9
4	-0.1	0.1	0.3	0.3
5	-0.1	0.8	-0.5	-0.2
6	-0.3	-0.2	-0.1	0.4
7	0.0	0.3	-0.5	-0.2
8	0.1	0.0	0.1	0.2
9	0.2	1.3	0.5	1.1

Geometrical harmonics for MBHDP01 and MBHSP03, defined as average measured values at the current of 3.5 kA during current ramp up and down, are shown in Table 1. The high order geometrical harmonics (n>3) in both single- and twin-aperture configurations are small except for the b_9 that slightly exceeds 1 unit. However, a_2 and b_3 are relatively large due to the deviations of "as-built" magnet geometry from the design cross-section.

CONCLUSION

Magnet *TF* and field harmonics were measured for the FNAL 1 m long twin-aperture 11 T dipole model MBHDP01. These data are in a good agreement with the experimental data for single-aperture dipole model MBHSP03 with the same coils. The high-order geometrical harmonics in both single- and twin-aperture configurations are small. Only a few low order harmonics are still relatively large and need to be reduced by optimizing the coil geometry and fabrication process. The effect of iron yoke saturation in the twin-aperture dipole MBHDP01 was measured up to 11 T. Good correlation of measured and calculated data was obtained using 3D ROXIE model based on the yoke length, cross-section geometry and magnetic properties. The coil magnetization effects related to the persistent currents in superconductor and eddy currents in the cable were discussed earlier and are well understood for the 11 T dipole.

ACKNOWLEDGMENT

The authors thank the staff of FNAL Technical Division for assistance with magnet design, fabrication and test.

REFERENCES

[1] A.V. Zlobin *et al.*, "Development of Nb_3Sn 11 T Single-Aperture Demonstrator Dipole for LHC Upgrades," in *Proc. of PAC'2011*, New York, NY, 2011, p. 1460.

[2] F. Savary *et al.*, "The 11 T Dipole for HL-LHC: Status and Plan", *IEEE Trans. on Appl. Supercond.*, vol. 26, no. 4, 2016, p. 4005305.

[3] A.V. Zlobin *et al.*, "11 T Twin-Aperture Nb_3Sn Dipole Development for LHC Upgrades," *IEEE Trans. on Appl. Supercond.*, vol. 25, no. 3, p. 4002209, 2015.

[4] A.V. Zlobin *et al*., "Quench performance of the first twin-aperture 11 T dipole for the LHC upgrades," in *Proc. of IPAC'2015*, Richmond, VA, 2015, p. 3361.
[5] M. Karppinen *et al*., "Design of 11 T Twin-Aperture Nb_3Sn Dipole Demonstrator Magnet for LHC Upgrades," *IEEE Trans. on Appl. Supercond*., vol. 22, no. 3, p. 4901504, 2012.
[6] A.V. Zlobin *et al*., "Fabrication and Test of a 1-m Long Single-Aperture 11T Nb_3Sn Dipole for LHC Upgrades", in *Proc. of IPAC'2013*, Shanghai, China, 2013, p. 3609.
[7] J. DiMarco *et al*., "Application of PCB and FDM Technologies to Magnetic Measurement Probe System Development", *IEEE Trans. on Appl. Supercond*., vol. 23, no. 3, p. 9000505, 2013.
[8] X. Wang *et al*., "Validation of finite-element models of persistent-current effects in Nb_3Sn accelerator magnets", *IEEE Trans. on Appl. Supercond*., vol. 25, no. 3, p. 4003006, 2015.
[9] ROXIE code for an electromagnetic simulation and optimization of accelerator magnets, `http://cern.ch/roxie`